Spectral prediction and dot surface estimation models for halftone prints

R. D. Hersch[1], F. Collaud[1], F. Crété[1], P. Emmel[2]

[1]Ecole Polytechnique Fédérale de Lausanne (EPFL), Switzerland

[2]Clariant International, Muttenz, Switzerland

ABSTRACT

We propose a new spectral prediction model as well as new approaches for modeling ink spreading which occurs when printing ink layer superpositions. The spectral prediction model enhances the classical Clapper-Yule model by taking into account the fact that proportionally more incident light through a given colorant surface is reflected back onto the same colorant surface than onto other colorant surfaces. This is expressed by a weighted mean between a component specifying the part of the incident light which exits through the same colorant as the colorant from which it enters (Saunderson corrected Neugebauer component) and a component specifying the part of the incident light whose emerging light components exit from all colorants, with a probability to exit from a given colorant equal to that colorant surface coverage (Clapper-Yule component). We also propose two models for taking into account ink spreading, a phenomenon which occurs when printing an ink halftone in superposition with one or several solid inks. Besides the physical dot gain present within a single ink halftone print, we consider in the first model the ink spreading which occurs when an ink halftone is printed on top of one or two solid inks. In the second more advanced model, we generalize this concept to ink halftones printed on top or below solid inks. We formulate for both ink spreading models systems of equations which allow to compute effective ink coverages as a combination of the individual ink coverages which occur in the different superposition cases. The new spectral prediction model combined with advanced ink spreading yields excellent spectral predictions for clustered-dot color halftone prints, both in the case of offset (75 to 150 lpi) and in the case of thermal transfer printers (50 to 75 lpi).

Keywords: Color printing, color halftone, spectral prediction model, dot gain, ink spreading, dot surface estimation, ink superposition conditions

1. INTRODUCTION

Since more than 50 years, attempts are being made to build models predicting the color of printed halftone images. To offer accurate predictions, the models need to take into account, at least to some extend, the phenomena determining the interactions of inks and paper and of light and halftone prints.

Many different phenomena influence the reflection spectrum of a color halftone patch printed on a diffusely reflecting substrate (e.g. paper). These phenomena comprise the surface (Fresnel) reflection at the interface between the air and the paper, light scattering and reflection within the substrate (i.e. paper bulk), and the internal (Fresnel) reflections at the interface between the paper and the air. The lateral scattering of light within the paper substrate and the internal reflections at the interface between the paper and the air are responsible for what is generally called the optical dot gain (also known as the "Yule-Nielsen" effect).

In addition, due to the printing process, the deposited ink surface coverage is generally larger than the nominal coverage, yielding a "physical" dot gain (sometimes also called "mechanical" dot gain). Effective ink surface coverages depend on the inks, on the paper, and also on the specific superpositions of the different inks.

At the present time, according to the literature [1], [2], among the existing spectral prediction models, only the well-known Yule-Nielsen model [3] seems to be used in practice. Most other spectral prediction models (see section 2) allow to explore various effects, but are either too complex or not accurate and comprehensive enough to be usable in practice.

The model we propose is an enhancement of the classical Clapper-Yule model which models optical dot gain of halftone prints by taking into account lateral scattering within the paper bulk and multiple internal reflections. Our model also takes into account physical dot surface coverages (physical dot gain) under all possible ink superposition conditions.

We have developed our prediction model by adding successive enhancements of the basic Clapper-Yule model. The benefits of each of these enhancements is verified by comparing measured halftone patch spectra and predicted spectra, for 729 patches, produced by generating all combinations of inks at nominal coverages 0%, 13%, 25%, 38%, 50%, 63%, 75%, 88% and 100%. We quantify the visual quality of color halftone patch predictions by converting measured and predicted spectra first to CIE-XYZ and then to CIE-LAB [4, pp. 8-12]. The Euclidian distance in CIE-LAB (1976) space gives a measure of the visually perceived distance between measured and predicted spectra. For deriving successive model improvements, we observe the predicted and measured spectra of patches where prediction and measurement disagree, try to give an explanation of the underlying phenomena (e.g. ink spreading) and propose an appropriate modeling step.

The measurements are carried out with a photospectrometer having a $45^o/0^o$ geometry, i.e. with a D65 light source illuminating the printed sample at an angle of 45° and a sensor capturing the reflected spectrum at 0° (normal to the printed sample).

2. EXISTING APPROACHES TO SPECTRAL COLOR PREDICTION

In early printing prediction models, the term "dot gain" encompasses both the physical dot gain (the enlargement of the printed dot) and the optical dot gain due to the lateral propagation of light (scattering within the paper bulk and internal reflections at the interface between paper and air). The Neugebauer model [5] predicts the CIE-XYZ color coordinates (also called tri-stimulus values) of a color halftone patch as the sum of the color coordinates of their individual colorants weighted by their fractional area coverages a_i. By replacing the color coordinates of colorants by their respective reflection spectra R_i, one obtains the spectral Neugebauer equations giving the predicted reflection spectra of printed color patches.

$$R(\lambda) = \sum_i a_i \cdot R_i(\lambda) \qquad (1)$$

In the case of independently printed cyan, magenta and yellow inks of respective coverages c, m, y, the fractional area coverages of the individual colorants are closely approximated by the Demichel equations [6] which give the probability of a point to be located within a given colorant area [1]

white: $\qquad a_w = (1-c) \cdot (1-m) \cdot (1-y)$

cyan: $\qquad a_c = c \cdot (1-m) \cdot (1-y)$

magenta: $\qquad a_m = (1-c) \cdot m \cdot (1-y)$

yellow: $\qquad a_y = (1-c) \cdot (1-m) \cdot y \qquad (2)$

red: $\qquad a_r = (1-c) \cdot m \cdot y$

green: $\qquad a_g = c \cdot (1-m) \cdot y$

blue: $\qquad a_b = c \cdot m \cdot (1-y)$

black: $\qquad a_k = c \cdot m \cdot y$

where a_w, a_c, a_m, a_y, a_r, a_g, a_b, a_k are the respective fractional areas of the colorants white, cyan, magenta, yellow, red (superposition of magenta and yellow), green (superposition of yellow and cyan), blue (superposition of magenta and cyan) and black (superposition of cyan, magenta and yellow). The Neugebauer model is a generalization of the Murray-Davis model [7] whose colorants are formed by only one ink and the paper white.

Since the Neugebauer model neither takes explicitly into account the lateral propagation of light within the paper bulk nor the internal reflections (Fresnel reflections) at the paper - air interface, its predictions are not accurate [8]. Yule and Nielsen [3] modeled the non-linear relationship between colorant reflection spectra and predicted reflectance by a power function, whose exponent n is fitted according to a limited set of measured patch reflectances:

$$R(\lambda) = \left(\sum_i a_i \cdot R_i(\lambda)^{\frac{1}{n}} \right)^n \qquad (3)$$

Ruckdeschel and Hauser [8] analyzed the Yule-Nielson model by modeling the lateral propagation of light within the paper bulk by a point spread function $H(x,y)$ The reflection spectrum R at the position (x,y) becomes

$$R(x, y) = T(x, y) \cdot R_p \cdot \int_{-\infty}^{\infty} \int_{-\infty}^{\infty} T(x', y')H(x - x', y - y')dx'dy' \qquad (4)$$

Light enters at all positions (x', y') located in the neighbourhood of (x, y), is attenuated by the ink transmittance $T(x', y')$, enters the paper bulk, propagates laterally with a fraction $H(x-x', y-y')$ reaching position (x, y), is attenuated according to the paper reflectance R_p, exits the paper bulk, is attenuated by the ink layer transmittance $T(x, y)$ and emerges at position (x, y).

Much research was carried out in building models by assuming various mathematical formulations of the point spread function $H(x, y)$. Both Gaussian line spread functions [9],[10] and exponential point spread functions were proposed [11], [12], [13]. Since the point spread function can also be viewed as a probability density, probability models were proposed to describe the lateral scattering of light within the paper bulk [14], [15], [16].

The models described by Eq. (4) assume that light traverses the ink layer, is laterally scattered and reflected by the paper, traverses a second time the ink layer (at a different position due to lateral scattering), and exits from the printed paper.

However, as known from optics, Fresnel reflections occur at a planar interface between two media of different indices of refraction. Since paper is formed by a network of layered cellulose fibers plus filler pigments, its index of refraction is different from the index of refraction of air. In addition, paper is often coated with a coating whose index of refraction is generally assumed to be 1.5.

In this context, we consider the Clapper-Yule model [17] which was developed for predicting the reflectance of photographic prints. The Clapper-Yule model has the advantage of modeling the specular reflections at the air-paper interface and the internal reflections (Fresnel reflections) at the paper-air interface. It assumes that lateral light propagation due to light scattering within the paper bulk is large compared with the period of the halftones. Therefore, the probability of light to exit from a given colorant is set equal to the colorant's fractional surface coverage.

Rogers [18] generalizes the Clapper-Yule model by modeling lateral scattering within the paper as a point spread function and by deducing the probabilities that light entering through a colorant n emerges from the coated paper through a colorant m, possibly traversing, due to multiple reflections, further intermediate colorants. Emmel and Hersch's unified model [19] also takes into account multiple internal reflections and modelizes lateral scattering probabilities by an exponential function with a circular symmetry and a strong radial decay.

Within the framework of their work on the reproduction of color images by custom inks, Stollnitz et. al. [20] predict the reflection spectra of solid colorants by using Kubelka's layering model [21] for combining the paper layer and the ink layers and by applying Saunderson's correction [22] in order to take into account multiple

reflections at the interface between the paper coating and the air. They predict halftone colors by combining the resulting solid colorant colors according to the Neugebauer equations, extended so as to account for dot gain and trapping.

3. THE BASIC CLAPPER-YULE SPECTRAL COLOR PREDICTION MODEL

Among the classical color prediction models [8], only the Clapper-Yule model [17] takes simultaneously into account halftone patterns and multiple internal reflections occurring at the interface between the coated paper and the air.

For introducing the Clapper-Yule model, we consider a single halftone ink layer with a fractional surface coverage a printed on a coated paper substrate (Fig. 1). Incident light has the probability a of reaching the paper substrate by passing through ink of transmittance $t(\lambda)$ and a probability $(1-a)$ of reaching the substrate without traversing the ink layer. Since r_s is the surface reflection at the air-paper interface, only portion $(1-r_s)$ actually enters the coated paper. The light reaching the paper substrate is reduced by a factor $(1-r_s)$ $(1-a+at)$. It is diffusely reflected by the paper substrate according to the paper substrate reflectance $r_g(\lambda)$. Travelling upwards, it traverses the coated paper with a portion a traversing the ink and a portion $1-a$ traversing an area free of ink. It is reflected at the coated paper-air interface according to reflection factor r_i (Fresnel reflection). A part $(1-r_i)$ of the light exits. At the first exit, the spectral attenuation of the incident light is therefore $(1-r_s)$ $r_g(1-r_i)$ $(1-a+at)^2$. The part reflected at the coated paper-air interface travels downward, is diffusely reflected by the paper and travels upwards again. At the second exit, the spectral attenuation is $(1-r_s)$ $r_g(1-r_i)$ $(1-a+at)^2$ r_i r_g $(1-a+at^2)$.

Specular reflection: r_s

1st reflection : $(1-r_s)$ $r_g(1-r_i)$ $(1-a+at)^2$

2nd reflection: $(1-r_s)$ $r_g(1-r_i)$ $(1-a+at)^2 \cdot$ r_i r_g $(1-a+at^2)$

nth reflection : $(1-r_s)$ $r_g(1-r_i)$ $(1-a+at)^2 \cdot$ $(r_i$ r_g $(1-a+at^2))^{n-1}$
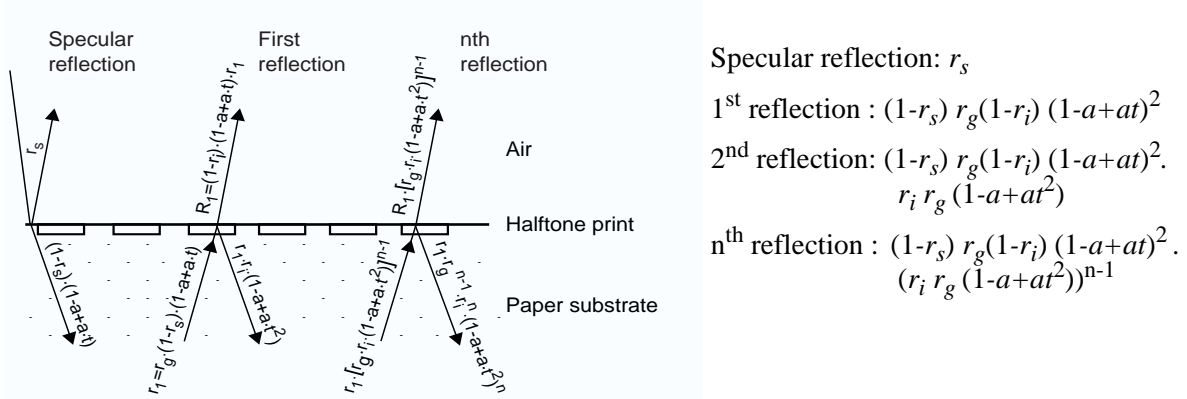
Fig. 1 Attenuation of light by multiple reflections on a halftone printed patch

With K giving the fraction of specular reflected light reaching the photospectrometer[1], and by considering the light emerging after 0, 1, 2,..., $n-1$ internal reflections (Fig. 1), we obtain the reflection spectrum

$$R(\lambda) = K \cdot r_s + ((1-r_s) \cdot (1-r_i) \cdot r_g \cdot (1-a+a \cdot t)^2) \cdot (1 + (r_i \cdot r_g \cdot (1-a+a \cdot t^2))$$

$$+ (r_i \cdot r_g \cdot (1-a+a \cdot t^2))^2 + \dots + (r_i \cdot r_g \cdot (a+a \cdot t^2))^{n-1}$$

For an infinite number of emergences (geometric series), we obtain

$$R(\lambda) = K \cdot r_s + \frac{(1-r_s) \cdot r_g \cdot (1-r_i) \cdot (1-a+a \cdot t)^2}{1 - r_g \cdot r_i \cdot (1-a+a \cdot t^2)} \qquad (5)$$

---

1. For a 45/0 degrees measuring geometry, we set K=0.

In the case of paper printed with 3 inks such as cyan, magenta and yellow, the coverages of the resulting 8 basic colorants, i.e. white[1], cyan, magenta, yellow, red, green, blue and black are obtained according to the Demichel equations (Eq. 2). By inserting the relative amounts of colorants a_i and their transmittances t_i in equation (5), we obtain for the predicted reflectance of a color patch printed with combinations of cyan, magenta and yellow inks

$$R(\lambda) = K \cdot r_s + \frac{(1 - r_s) \cdot r_g \cdot (1 - r_i) \cdot \left(\sum_{j=1}^{8} a_j \cdot t_j \right)^2}{1 - r_g \cdot r_i \cdot \sum_{j=1}^{8} a_j \cdot t_j^2} \quad (6)$$

Both the specular reflection r_s and the internal reflection r_i depend on the refraction indices of the air ($n_1=1$) and of the coated paper ($n_2=1.5$), independently of whether the considered surface is white or printed (the ink is located within the coated paper surface). According to the Fresnel equations [23], for collimated light at an incident angle of 45°, the specular reflection factor is $r_s=0.05$. With light diffusely reflected by the paper (Lambert radiator), according to Judd [24], by summing up the contributions at all reflection angles, one obtains the internal reflection factor $r_i=0.6$.

To put the model into practice, we deduce from (5) the internal reflectance spectrum r_g of a blank paper by setting the ink coverage $a=0$. R_w is the measured blank paper reflectance.

$$r_g = \frac{R_w - K \cdot r_s}{1 + (1 - K) \cdot r_i \cdot r_s + r_i \cdot R_w - r_s - r_i} \quad (7)$$

We then extract the transmittance of the individual inks and ink combinations $t_w, t_c, t_m, t_y, t_r, t_g, t_b, t_k$ by inserting in eq. 5 as $R(\lambda)$ the measured solid (100%) ink coverage reflectance R_i and by setting the ink coverage $a=1$.

$$t_i = \sqrt{\frac{R_i - K \cdot r_s}{r_g \cdot r_i \cdot (R_i - K \cdot r_s) + r_g \cdot (1 - r_i) \cdot (1 - r_s)}} \quad (8)$$

We must also take a possible physical dot gain into account. For each ink, we fit according to Clapper-Yule (eq. 5) the unknown physical coverages of the measured single ink patches at nominal coverages of for example 10%, 20%, ... 90% by minimizing the sum of square differences between measured spectra and predicted spectra (similar to the dot area optimization proposed by Balasubramanian [2]). For the basic Clapper-Yule model, fitted single ink surface coverages are lower than the nominal surface coverages, i.e. we obtain a negative dot gain (Fig. 2a). This is due to the fact that spectra predicted by the Clapper Yule model are darker than the corresponding measured spectra. The fitted negative dot gain tends to bring both spectra to the same levels, i.e. the predicted and measured spectra intersect each other (Fig. 2b).
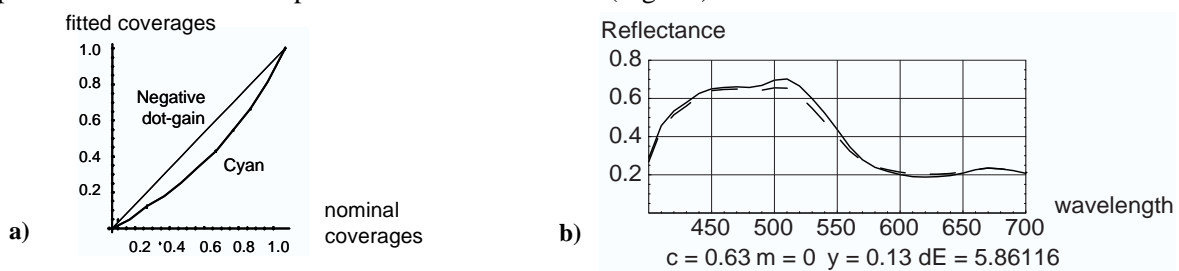
Fig. 2 (a) Negative dot gain induced by the too dark Clapper-Yule predictions and (b) corresponding measured (continuous) and predicted (dashed) reflection spectra

1. The internal transmittance t_w of white (no ink) is 1 at each wavelength

In order to set a base line for improvements, we test the accuracy of the basic Clapper-Yule model taking into account single ink dot gain (i.e. single ink physical dot surface optimization, see [2], section 4) by printing at the considered lineatures a set of 729 patches. Lineatures represent the screen element frequencies and are expressed in lines per inch (lpi). These patches are produced by generating all combinations of cyan, magenta, yellow ink superpositions at nominal coverages 0%, 13%, 25%, 38%, 50%, 63%, 75%, 88% and 100%. Measured and predicted spectra are converted to CIE-LAB values and the resulting error is computed. With the Clapper-Yule model, for offset prints at a lineature of 150 lpi, a mean error of $\Delta E = 3.95$ is obtained, the maximal error is 10.98 and 352 values have a ΔE greater than 4. At a lineature of 75 lpi, a mean error of $\Delta E = 4.49$ is obtained, the maximal error is 9.19 and 438 values have a ΔE greater than 4.

4. A NEW SPECTRAL COLOR PREDICTION MODEL

Spectra predicted by the Clapper-Yule model (without the negative dot gain compensation) are too dark, because according to the measured modulation transfer function of paper [25], light does not travel significantly more than 1/10 of a mm within coated paper. With screen frequencies between 20 to 60 lines per cm (50 to 150 lines per inch), the probability that light having entered at a position having a certain ink color exits from a position of the same color is higher than the coverage of that ink color. Therefore, the basic assumption of the Clapper-Yule model, i.e. the probability of light exiting from a specific colorant being equal to that colorant coverage, is not fulfilled.

In order to enhance the basic Clapper-Yule model, we assume that a certain part b of the incident light through a given colorant is reflected back and exits from the same colorant. The part $(1-b)$ of the incoming light behaves in the same way as in the basic Clapper-Yule model described above. We also make the simplifying assumption that the part b of the incident light which is reflected onto the same colorant also exits from the same colorant after one or several reflections at the paper-air interface.

Taking again multiple reflections into account, the attenuation of the part of the incoming light exiting from the same ink color (either no ink or ink with coverage a) at the first exit is

$$(1 - r_s) \cdot r_g \cdot (1 - r_i) \cdot (1 - a + a \cdot t^2)$$

at the 2nd exit, the attenuation is

$$(1 - r_s) \cdot r_g \cdot (1 - r_i) \cdot (r_g \cdot r_i) \cdot (1 - a + a \cdot t^4)$$

and at the nth exit the attenuation is

$$(1 - r_s) \cdot r_g \cdot (1 - r_i) \cdot (r_g^{n-1} \cdot r_i^{n-1})[(1 - a) + a \cdot t^{2n}]$$

The sum of all light components that exit after an infinite number of reflections yields the spectrum

$$R(\lambda) = (1 - r_s) \cdot (1 - r_i) \cdot \left(\frac{(1 - a) \cdot r_g}{1 - (r_i \cdot r_g)} + \frac{a \cdot r_g \cdot t^2}{1 - (r_i \cdot r_g \cdot t^2)} \right) \qquad (9)$$

Equation (9) reflects the application of the Saunderson correction [22] accounting for multiple internal reflections at the paper-air interface: the first term models the paper without ink (internal reflectance r_g) and the second term the paper printed with solid ink (internal reflectance $r_g \cdot t^2$). Equation (9) can also be conceived as a Saunderson corrected Murray-Davis equation.

The enhanced model (eq. 10) comprises a part b of light propagated along short and middle distances (eq. 9) and a part $(1-b)$ of the light propagated along long distances (eq. 6).

$$R(\lambda) = K \cdot r_s + (1 - r_s) \cdot r_g \cdot (1 - r_i) \cdot \left[b \cdot \sum_{j=1}^{8} \frac{a_j \cdot t_j^2}{1 - r_i \cdot r_g \cdot t_j^2} + (1 - b) \cdot \frac{\left(\sum_{j=1}^{8} a_j \cdot t_j \right)^2}{1 - r_g \cdot r_i \cdot \sum_{j=1}^{8} a_j \cdot t_j^2} \right] \quad (10)$$

In equation (10), the part weighted by factor b represents the Saunderson corrected Neugebauer component (Murray-Davis equation extended to multiple colorants) and the part weighted by factor (1-b) represents the Clapper-Yule component.

In order to obtain factor b for a given lineature, we establish the prediction accuracy for 729 patches and select the value for b which yields the smallest mean error between the predicted and measured reflection spectra. For cyan, magenta, yellow offset printing with screens mutually rotated by 30° and a screen frequency of 75 lines per inch, the fraction b yielding the smallest mean error for all considered test patches is $b=0.6$. Under the same conditions, at 150 lines per inch, we obtain a smallest mean error at $b=0.1$, i.e. the enhanced spectral prediction model is very close to the classical Clapper-Yule model.

6. PHYSICAL DOT COVERAGES ACCOUNTING FOR INK SPREADING

In offset printing, trapping, i.e. the decrease in thickness of ink layers when two or more inks are printed one on top of another is generally considered to be a problem [26, pp. 103-105]. Our model automatically takes care of trapping by computing the internal transmittances of the red, green, blue and black colorants from spectral reflection measurements according to equation (8). However, we observed an ink spreading phenomenon when a second ink halftone is printed over a first solid ink or when a third ink halftone is printed on top of two solid inks. Similarly to the physical dot gain of a printed single ink halftone patch, ink spreading enlarges the effective surface of a printed dot (Figure 3) and tends to lower the resulting reflection spectrum, i.e. it yields slightly darker colors.
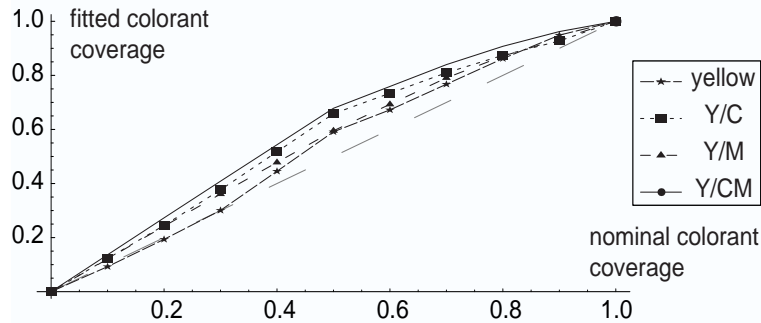
Fig. 3 Tone reproduction curves for yellow alone, yellow over solid cyan, yellow over solid magenta and yellow over solid cyan and magenta

We develop a first model for computing effective surface coverages (physical coverages) which accounts for ink spreading. This first model assumes that when printing two successive ink layers one on top of another, ink spreading only occurs on the top layer. The top layer does not influence the effective surface coverage of the ink layer beneath it.

Let us consider a printing process where offset inks are printed by first depositing cyan, then magenta and then yellow. We therefore fit the respective ink spreaded coverages of magenta over solid (i.e. 100%) cyan $f_{cm}(m)$, yellow over solid cyan $f_{cy}(y)$, yellow over solid magenta $f_{my}(y)$ and yellow over solid cyan and magenta $f_{cmy}(y)$

by minimizing the square differences between measured spectra and spectra predicted according to equation (10), for a number of nominal surface coverages, e.g. 25%, 50%, and 75%. The continuous functions $f_{uv}(v)$ mapping nominal to effective coverages are obtained by linear interpolation between points formed by pairs of nominal and fitted effective coverage values (see Fig. 3).
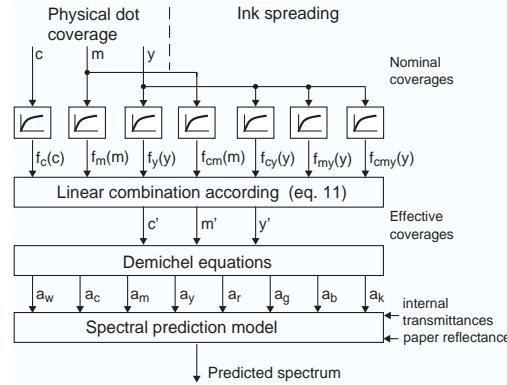
Fig. 4 Spectral prediction model with dot gain and ink spreading when an ink is printed on top of another ink

In front of our new spectral prediction model, we introduce a stage taking into account effective surface coverages induced by dot gain and ink spreading (Fig. 4). An input color with nominal coverages *cmy* is converted to an intermediate color with effective coverages *c'm'y'* obtained as a weighted sum of dot gain and ink spreading contributions.

The weighting coefficients are given by the respective effective colorant coverages.

$$c' = f_c(c) \qquad\qquad\qquad \text{; effective surface coverage of cyan only} \qquad\qquad (11)$$

$$m' = f_m(m)\,(1-c') + f_{cm}(m)\,c' \qquad \text{; magenta alone and magenta on top of solid cyan (blue)}$$

$$y' = f_y(y)\,(1-c')\,(1-m') \qquad\qquad\qquad\qquad \text{; yellow alone}$$
$$\quad + f_{my}(y)\,(1-c')\,m' + f_{cy}(y)\,c'\,(1-m') + f_{cmy}(y)\,c'\,m' \; \text{; yellow on top of solid magenta (red), of solid cyan}$$
$$\text{(green) and of solid cyan \& magenta (black)}$$

The performance of this simple ink spreading model is illustrated by the prediction accuracies in the second row ("dot gain and ink spreading according to the print order") of the tables shown in the Appendix, both for the Clapper-Yule model and for our new spectral prediction model. The increase in prediction accuracy, compared with standard single ink dot gain optimization is important: for offset prints, the mean difference between predicted and measured spectra, expressed in CIE-LAB is reduced by 25% to 50%. This increase in prediction accuracy is true both for the Clapper-Yule model and for the new spectral prediction model.

7. EFFECTIVE COVERAGES IN INK LAYER SUPERPOSITIONS: ADVANCED MODEL

A more advanced model for computing the effective surface coverages in layer superpositions relies on the assumption that when a halftone layer is printed either beneath or on top of a solid layer, its effective surface coverage is modified.

We separately model as functions of nominal coverages (a) the surface coverages of single ink halftones (b) the surface coverages of single ink halftones superposed with one solid ink and (c) the surface coverages of single ink halftones superposed with two solid inks. We then appropriately weight these different surface coverage functions and obtain the resulting effective coverage of each ink as a function of the nominal ink surface coverages. During calibration of the model, effective coverage values defining the different surface coverage functions are fitted by minimizing the sum of square differences between measured and predicted reflection spectra.

The functions describing effective surface coverages of single ink halftones printed in superposition with paper white, one solid ink or two solid inks are obtained by fitting effective surface coverages (e.g. at 25%, 50% and 75% nominal coverages) of an ink using the spectral prediction model given by equation (10). This allows to associate effective (fitted) surface coverages to the nominal surface coverages, for a limited set of halftone patches of each ink, in each ink superposition condition. By linear interpolation between the so obtained effective coverages, we obtain the function mapping nominal to effective surface coverages for each ink and for each ink superposition condition.

Let us consider 3 inks i_1, i_2 and i_3 with nominal coverages c_1, c_2 and c_3. The "dot gain" functions mapping nominal coverages to effective coverages for single ink halftones are $f_1(c_1)$, $f_2(c_2)$ and $f_3(c_3)$. The "ink spreading" functions mapping nominal coverages of an ink to effective coverages of that ink, for single ink halftones superposed with a second solid ink or single ink halftones superposed with two solid inks are:

- for ink i_1 of coverage c_1 superposed with solid ink i_2 : $f_{21}(c_1)$,
- for ink i_1 of coverage c_1 superposed with solid ink i_3 : $f_{31}(c_1)$,
- for ink i_2 of coverage c_2 superposed with solid ink i_1 : $f_{12}(c_2)$,
- for ink i_2 of coverage c_2 superposed with solid ink i_3 : $f_{32}(c_2)$,
- for ink i_3 of coverage c_3 superposed with solid ink i_1 : $f_{13}(c_3)$,
- for ink i_3 of coverage c_3 superposed with solid ink i_2 : $f_{23}(c_3)$,
- for ink i_1 of coverage c_1 superposed with solid inks i_2 and i_3 : $f_{231}(c_1)$,
- for ink i_2 of coverage c_2 superposed with solid inks i_1 and i_3 : $f_{132}(c_2)$,
- for ink i_3 of coverage c_3 superposed with solid inks i_1 and i_2 : $f_{123}(c_3)$.

In the case of three inks, these 12 functions are obtained by fitting 36 patches, i.e. 3 patches (25%, 50% and 75% nominal coverages) per function.

Fig. 5 gives an example of effective surface coverages (round black dots at nominal coverages of 10%, 20%,.., 90%) fitted according to the disclosed spectral prediction model, for wedges printed alone (left column), for wedges printed in superposition with one solid ink (2nd and 3rd columns) and for wedges printed in superposition with two solid inks (right column). Wedges of cyan are shown in the first row, wedges of magenta in the second row and wedges of yellow in the third row. One can see for example that the effective surface coverages of magenta (2nd row) depend if magenta is printed alone (2nd row, 1st column), in superposition with cyan (2nd row, 2nd column), in superposition with yellow (2nd row, 3rd column) or in superposition with cyan and magenta (2nd row, 4th column). One can observe the same phenomenon for the yellow wedges (3rd row).
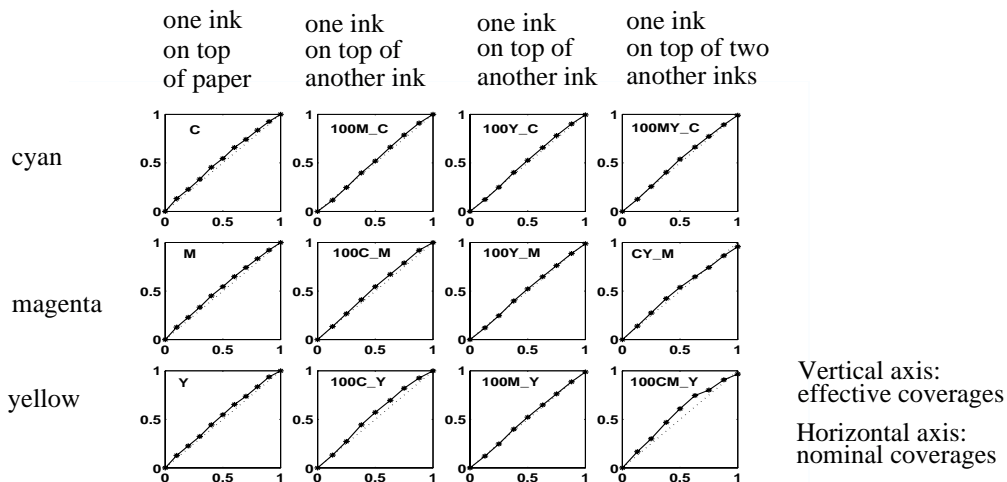
Fig. 5 Example of effective ink coverages for different superposition conditions (offset prints)

Once surface coverages are fitted according to the spectral prediction model, linearly interpolating between these surface coverages (in Fig. 5, dark line segments connecting the round black dots) yields the functions mapping nominal to effective (i.e. physical) surface coverages for ink halftones printed in different superposition conditions.

For a nominal halftone patch of coverages c_1, c_2 and c_3, it is necessary, for each ink i_k, to weight the contributions of the corresponding mapping functions f_k, f_{lk}, f_{mk}, and f_{lmk}. The weighting functions depend on the effective coverages of the considered ink alone, of the considered ink in superposition with a second ink and of the considered ink in superposition with the two other inks. For the considered system of 3 inks i_1, i_2 and i_3 with nominal coverages c_1, c_2 and c_3 and effective coverages c_1', c_2' and c_3', assuming that inks are printed independently of each other, by computing the relative weight, i.e. the relative surface of each superposition condition, we obtain the system of equations (12). In analogy with Demichel's equations (2), the proportion (relative effective surface) of a halftone patch printed with ink i_1 of coverage c_1 on paper white is $(1-c_2')(1-c_3')$. The proportion of the same patch printed on top of solid ink i_2 is $c_2'(1-c_3')$, the proportion of the same patch printed on top of solid ink i_3 is $(1-c_2')c_3'$ and the proportion of the same patch printed on top of solid inks i_2 and i_3 is c_2' c_3'. We obtain the following system of equations:

$$c_1' = f_1(c_1)(1-c_2')(1-c_3') + f_{21}(c_1)c_2'(1-c_3') + f_{31}(c_1)(1-c_2')c_3' + f_{231}(c_1)c_2'c_3'$$

$$c_2' = f_2(c_2)(1-c_1')(1-c_3') + f_{12}(c_2)c_1'(1-c_3') + f_{32}(c_2)(1-c_1')c_3' + f_{132}(c_2)c_1'c_3' \qquad (12)$$

$$c_3' = f_3(c_3)(1-c_1')(1-c_2') + f_{13}(c_3)c_1'(1-c_2') + f_{23}(c_3)(1-c_1')c_2' + f_{123}(c_3)c_1'c_2'$$

This system of equations can be solved iteratively: one starts by setting initial values of c_1', c_2' and c_3' equal to the respective nominal coverages c_1, c_2 and c_3. After one iteration, one obtains new values for c_1', c_2' and c_3'. These new values are used for the next iteration. After a few iterations, typically 4 to 5 iterations, the system stabilizes and the obtained coverages c_1', c_2' and c_3' are the effective coverages. The system of equations (eq. 12) allows therefore to compute combined effective ink surface coverages (physical dot sizes) resulting from the combination of elementary ink surface coverages present in different superposition conditions.

The effective colorant coverages a_1', a_2', .. a_8' are obtained from the effective coverages c_1', c_2' and c_3' of the inks according to the Demichel equations (eq. 2). With the spectral prediction model (eq. 10) and by taking into account the combined effective ink coverages (physical dot coverages), we obtain a further improvement in prediction accuracy (see Tables in Appendix). CIE-LAB prediction errors are reduced by another 10% to 40%, compared with the simple ink spreading model (ink spreading only on top of a single ink) described in section 6.

For the same offset prints as before (Table 1 in the Appendix), thanks to the new spectral prediction and the advanced ink spreading models, at 75 lpi, with parameter b=0.6, a mean error between predicted reflection spectra and measured reflection spectra (in the present case 729 spectra) of ΔE =1.35 was obtained, the maximal error is ΔE=3.92 and no value has a ΔE greater than 4. At 150 lpi, with parameter b=0.1, a mean error between predicted reflection spectra and measured reflection spectra (729 spectra) of ΔE =1.60 was obtained, the maximal error is ΔE=4.56 and 8 values have a ΔE greater than 4.

Although the model is presented here for the combination of any freely chosen set of three inks, it has been extended to four inks. This extension is straightforward: it requires to extend the Demichel equations (eq. 2), the spectral prediction model (eq. 10) and the equations allowing to compute the effective surface coverages in different superposition conditions (eq. 12).

In contrast to Stollnitz's model [20], our model only fits effective dot sizes when printed alone or in combination with other inks (physical dot gain, ink spreading), but predicts spectra (36 components). It does not fit neither the transmission spectra of any of the inks nor the reflection spectrum of paper. All internal spectra are calculated from measured spectra, according to the model. Therefore the model reflects at least to a certain extent the underlying physical phenomena.

8. APPLICATION OF THE MODEL

The proposed spectral prediction model together with the methods of computing effective surface coverages was applied to offset and thermal transfer printing, at various lineatures, for the cyan, magenta and yellow inks. Classical clustered-dot halftoning was used, with screens mutually rotated by 30°. We present the prediction accuracies when printing with cyan, magenta and yellow inks on offset (Komori Lithrone 26) at lineatures of 75 and 150 lpi and on a thermal transfer wax printer (Alps MD-5000 at 600 dpi) at lineatures of 50, 75 and 100 lpi. The tables in the Appendix give the mean prediction errors (in terms of the CIELAB 1976 ΔE values), the maximal prediction error and the number of patches having an error larger than $\Delta E = 4$. For fitting the effective dot surfaces, only 25%, 50% and 75% nominal coverages were used, yielding in case of single ink dot surface optimization (dot gain) 3x3=9 patches, in case of ink spreading when printed on *top* of one or two inks 3x7=21 patches (eq. 11) and in case of ink spreading for all superposition conditions 3x12= 36 patches (eq. 12). In addition, the reflectances of the paper white and of solid patches of all ink and ink combinations are measured (8 patches). The model is tested on 729 patches, comprising all nominal coverage combinations at 0%, 13%, 25%, 38%, 50%, 63%, 75%, 88% and 100%.

The prediction results clearly show that the *new spectral prediction model* as well as the two *ink spreading* models improve the prediction performance. One can also clearly see that combined with the new spectral prediction model, the two ink spreading models bring considerable improvements in prediction accuracy. The ink spreading models also bring an improvement to the classical Clapper-Yule model, but as shown by the results obtained with the Alps thermal transfer printer (Appendix, Table 2, 50 and 75 lpi), the improvement is less pronounced than with the new spectral prediction model. The proposed models provide excellent predictions (mean CIE-LAB prediction error below $\Delta E = 1.6$) as long as the printed dot is stable (e.g. offset at 75 and 150 lpi, thermal transfer prints at 50 and 75 lpi). When the printed dot becomes somehow unstable (e.g. Table 2, Alps thermal transfer printer at 100 lpi), the proposed models still improve the prediction accuracy compared with Clapper-Yule, but provide a lower accuracy (mean ΔE of 2.5 at 100 lpi for the thermal transfer Alps printer).

The results also confirm that the factor b giving the relative weights of respectively the Saunderson corrected Neugebauer and of the Clapper-Yule components of the spectral prediction model is related to the screen lineature. At a higher lineature, the ratio of lateral light scattering to screen element period is higher and therefore, the weight of the Clapper-Yule component within the new spectral prediction model becomes larger. Therefore, factor b which is proportional to the weight of the Saunderson corrected Neugebauer component becomes smaller (Table 2, second line).

9. CONCLUSIONS

We propose a new spectral prediction model which represents a considerable progress compared with the classical Clapper-Yule model by taking into account the fact that proportionally more incident light through a given colorant surface is reflected back onto the same colorant surface than onto other colorant surfaces. This is expressed by a factor b which specifies the part of the incident light which must exit through the same colorant as the colorant from which it entered (i.e. lateral light propagation is short compared with the screen element period) and a factor ($1-b$) specifying the part of the incident light whose emerging light components may also exit from other colorants, with a probability to exit from a given colorant equal to that colorant surface coverage (lateral light propagation is middle to large, compared with the screen element period). One can conceive the proposed spectral prediction model as a weighted mean between the Clapper-Yule and the Saunderson corrected Neugebauer model components.

We also propose two models for taking into account *ink spreading*, a phenomenon which occurs when printing an ink halftone in superposition with one or several solid inks. Besides the physical dot gain present within a single ink halftone print, we consider in the first model the ink spreading which occurs when an ink halftone is

printed on *top* of one or two solid inks. In the second more advanced model, we generalize this concept to ink halftones printed on top or *below* solid inks. We formulate for both models systems of equations which allow to compute effective ink coverages as combinations of individual ink coverages which occur in the different superposition conditions.

For model calibration, i.e. the establishment of the functions mapping nominal to effective surface coverages in the different superposition conditions, effective coverage values are fitted by minimizing the sum of square differences between measured and predicted reflection spectra. In the case of three inks (cyan, magenta and yellow), for the advanced ink spreading model, the calibration set can be as small as 44 samples. It comprises the paper white, seven solid ink samples and 36 halftone samples yielding 36 fitted surface coverages for the 12 linearly interpolating functions mapping nominal to effective surface coverages.

Both the new spectral prediction model and the new methods of estimating effective coverages (dot sizes) considerably improve the predictions. Tests were carried out with 729 color patches covering the complete gamut of the output device. For offset prints, at 150 lpi (see Table 1, Appendix), the new spectral prediction model and the advanced method for computing effective coverages improves the standard Clapper-Yule predictions by reducing the mean CIE-LAB (1976) error between predicted and measured spectra by a factor of 2.4 (from $\Delta E = 3.95$ to $\Delta E = 1.60$). At 75 lpi, the Clapper-Yule mean prediction error is reduced by a factor of 3.3 (from $\Delta E = 4.49$ to $\Delta E = 1.35$). Errors below to $\Delta E = 1.5$ cannot be reduced further, since they correspond to the colorimetric variations which occur when printing identical patches at different locations of the same printed page.

Since our new model only fits surface coverages when inks are printed alone or in superposition with other inks, but predicts spectra (36 components), it seems to reflect, at least to a certain extent, the underlying physical phenomena. However, further efforts are needed to verify that indeed the computed effective surface coverages correspond to physical dot areas.

At the present time, the spectral prediction model together with the ink spreading modelization yield excellent results for clustered dots, in the case of offset and thermal transfer technologies. Further research is needed for obtaining similar results for dispersed-dot or error-diffusion halftoning algorithms, as well as for ink-jet and electrophotographic printers.

REFERENCES

1. D.R.Wyble, R.S. Berns, A Critical Review of Spectral Models Applied to Binary Color Printing, *Journal of Color Research and Application*, Vol. 25, No. 1, 4-19, (2000)
2. R. Balasubramanian, Optimization of the spectral Neugebauer model for printer characterization, *Journal of Electronic Imaging*, Vol. 8, No. 2, 156-166 (1999)
3. J.A.C. Yule, W.J. Nielsen, The penetration of light into paper and its effect on halftone reproductions, Proc. *TAGA*, Vol. 3, 65-76 (1951),
4. H.R. Kang, *Color Technology for Electronic Imaging Devices*. SPIE Optical Engineering Press (1997).
5. H.E.J. Neugebauer, Die theoretischen Grundlagen des Mehrfarbendrucks. *Zeitschrift fuer wissenschaftliche Photographie,* Vol. 36, 36-73, (1937), reprinted in *Neugebauer Seminar on Color Reproduction,* SPIE Vol-1184,194-202 (1989)
6. M.E. Demichel, 1924. Procédé, Vol. 26, 17-21.
7. A. Murray, Monochrome reproduction in photoengraving, J. Franklin Institute, Vol. 221, 721-724 (1936)
8. H.R. Kang, Applications of color mixing models to electronic printing. *Journal of Electronic Imaging,* Vol. 3, No. 3, 276-287 (1994)
9. F.R. Ruckdeschel, O.G. Hauser, Yule-Nielsen in printing: a physical analysis, *Applied Optics*, Vol. 17, No. 21, 3376-3383 (1978)
10. J.A.C. Yule, D.J. Howe, J.H. Altman, The effect of the spread function of paper on halftone reproduction, *TAPPI Journal,* Vol. 50, No. 7, 337-344, (1967)

11. H. Wakeshima, T. Kunishi, S. Kaneko, Light Scattering in Paper and its Effect on Halftone Reproduction, *Journal of the Optical Society of America*, Vol. 58, 272-273 (1968)

12. P. G. Engeldrum, B. Pridham, Application of Turbid Medium Theory to Paper Spread Function Measurements, *Proc. TAGA Proc.*, Vol. 47, 339-352 (1995)

13. S. Gustavson, Color Gamut of Halftone Reproduction, *Journal of Imaging Science and Technology*, Vol. 41, No. 3, 283-290 (1997)

14. J. S. Arney, A Probability Description of the Yule-Nielsen Effect I, *Journal of Imaging Science and Technology*, Vol. 41, No. 6, 633-636 (1997)

15. G. Rogers, Optical Dot Gain: Lateral Scattering Probabilities, *Journal of Imaging Science and Technology*, Vol. 42, No. 4, 341-345, (1998)

16. L. Yang, S. Gooran, B. Kruse, Simulation of Optical Dot Gain in Multichromatic Tone Production, *Journal of Imaging Science and Technology*, Vol. 45, No. 2, 198-204 (2001)

17. F.R. Clapper, J.A.C Yule, The effect of multiple internal reflections on the densities of halftone prints on paper, *Journal of the Optical Society of America*, Vol. 43, 600-603 (1953)

18. G. Rogers, A Generalized Clapper-Yule Model of Halftone Reflectance. *Journal of Color Research and Application,* Vol. 25, No. 6, 402-407 (2000)

19. P. Emmel, R.D. Hersch, A Unified Model for Color Prediction of Halftoned Prints, *Journal of Imaging Science and Technology*, Vol. 44, No. 4, 351-359 (2000)

20. E.J. Stollnitz, V. Ostromoukhov, D. Salesin, Reproducing Color Images Using Custom Inks. *Proc. SIGGRAPH 1998*, in *Computer Graphics Proceedings*, Annual Conference Series, ACM Press,219-228 (1998)

21. P. Kubelka, New contributions to the optics of intensely light-scattering material, part II: Non-homogeneous layers. *Journal of the Optical Society of America,* Vol. 44, 330-335 (1954)

22. J.L. Saunderson, Calculation of the color pigmented plastics, *Journal of the Optical Society of America*, Vol. 32, 727-736 (1942)

23. E. Hecht, *Schaum's Outline of Optics*, Mc-Graw-Hill (1974)

24. D.B. Judd, Fresnel reflection of diffusely incident light, *Journal of Research of the National Bureau of Standards,* Vol. 29, 329-332 (1942)

25. S. Inoue, N. Tsumara, Y. Miyake, Measuring MTF of Paper by Sinusoidal Test Pattern Projection. *Journal of Imaging Science and Technology*, Vol. 41, No. 6, 657-661 (1997)

26. H. Kipphan, *Handbook of Print Media*. Springer-Verlag, (2001)

APPENDIX: PREDICTION ACCURACIES

TABLE 1. Prediction accuracy for offset cyan, magenta and yellow halftone prints

Offset printing 729 test samples	Max ΔE	Mean ΔE	# samples $\Delta E > 4$	Max ΔE	Mean ΔE	# samples $\Delta E > 4$
	75 lpi, b=0.6			150 lpi, b=0.1		
Clapper-Yule with single ink dot-gain only	9.19	4.49	438	10.98	3.95	352
Clapper-Yule, dot-gain and ink spreading according to print order	7.87	2.76	162	4.65	2.06	20
Clapper-Yule, dot gain and ink spreading for all superposition conditions	8.05	2.44	129	4.23	1.70	6
New spectral prediction model, with single ink dot-gain only	4.59	2.13	7	10.15	3.55	292
New spectral prediction model, dot-gain and ink spreading according to print order	3.79	1.57	0	4.70	1.95	14
New spectral prediction model, dot-gain and ink spreading for all superposition conditions	3.92	1.35	0	4.56	1.60	8

TABLE 2. Prediction accuracy for thermal transfer color halftone prints

Thermal transfer (ALPS MD-5000) 729 test samples	Max ΔE	Mean ΔE	# samples ΔE>4	Max ΔE	Mean ΔE	# samples ΔE>4	Max ΔE	Mean ΔE	# samples ΔE>4
	50 lpi, b=0.5			75 lpi, b=0.4			100 lpi, b=0.3		
Clapper-Yule with single ink dot-gain only	7.21	2.96	170	7.59	3.34	241	8.16	3.30	224
Clapper-Yule, dot-gain and ink spreading according to print order	7.42	2.63	103	7.18	3.07	173	7.73	3.04	175
Clapper-Yule, dot gain and ink spreading for all superposition conditions	7.74	2.51	108	7.06	2.38	95	7.73	2.84	146
New spectral prediction model, with single ink dot-gain only	6.63	2.34	86	7.73	3.02	190	7.33	3.21	223
New spectral prediction model, dot-gain and ink spreading according to print order	6.63	2.14	54	7.75	2.90	174	7.51	2.99	168
New spectral prediction model, dot-gain and ink spreading for all superposition conditions	4.56	1.50	5	5.01	1.51	13	6.79	2.50	78